J. Membrane Biol. 147, 275–281 (1995)

The Journal of
Membrane
Biology

Spatial Organization of Transport Domains and Subdomain Formation in the Plasma Membrane of *Chara corallina*

J. Fisahn,*[,1] W.J. Lucas[2]

[1]Institut für Genbiologische Forschung GmbH, Ihnestr. 63, 14195 Berlin, Germany
[2]Department of Botany, University of California, Davis, CA 95616

Received: 19 October 1994/Revised: 15 June 1995

Abstract. Pattern formation mechanisms in developing organisms determine cellular differentiation and function. However, the components that interact during the manifestation of a spatial pattern are in general unknown. Characean algae represent a model system to study pattern formation. These algae develop alternating acid and alkaline transport domains that influence the pattern of growth. In the present study, it will be demonstrated that a diffusion mechanism is implicated in acid and alkaline domain formation and this growth pattern. Experiments on the characean growth pattern were performed that resulted in pronounced, however, unpredictable modifications in the original pattern. A major component involved in this pattern-forming mechanism emerged from the nonlinear kinetics of the H^+-ATPase that is located in the plasma membrane of these algae. Based on these kinetics, a mathematical model was developed and numerically analyzed. As a result, the contribution of a diffusional component to the characean acid/alkaline pattern appeared most likely.

Key words: *Chara* — H^+-ATPase — Spatial organization — Transport domain

Introduction

During cell growth, characean cells develop alternating acid and alkaline membrane transport domains when exposed to light (Spear, Barr & Barr, 1969; Smith & Walker, 1976; Lucas, 1982, 1983; Fisahn & Lucas, 1992). This segmentation provides the basis for a cellular elongation mechanism that is limited to the acid regions (Metraux, Richmond & Taiz, 1980). The differentiation into acid and alkaline transport domains is generated by transport proteins which are located in the plasma membrane of these algal cells. While H^+ export mediated by the H^+-ATPase dominates the acid areas, H^+ import is observed in the alkaline regions (Spanswick, 1981). Recent studies indicated that a common transport protein facilitates the currents associated with these acid and alkaline transport domains (Fisahn, Hansen & Lucas, 1992).

Little is known about the processes and signals involved in the generation of a spatial biological pattern such as the acid and alkaline regions of *Chara* (Quatrano, 1978, 1990; Fisahn & Lucas, 1990*b*; Green, 1992; Wagner, Brian & Quatrano, 1992; Goodner & Quatrano, 1993). Genes themselves are not capable of generating a spatial growth pattern. However, the products of some genes might function in spatial domain organization. Several mechanisms have been analyzed in terms of their capability to induce a defined cellular polarity. One of these hypotheses implies the effect of transport proteins in pattern formation around the zygotes of the marine brown alga *Fucus* (Jaffe, 1977, 1981; Jaffe & Nuccitelli, 1977). In particular, an asymmetric distribution of Ca^{2+} channels is assumed to give rise to Ca^{2+} currents between the apical and rhizoidal pole of these embryos. However, the mechanisms that induce these asymmetric distributions of Ca^{2+} channels have not been identified. Similar to the acid and alkaline regions of *Chara,* light is a prerequisite to pattern formation in these marine algae (Jaffe, 1981; Goodner & Quatrano, 1993).

Often morphogens are thought to be involved in the generation of spatial information. In particular, morphogen distributions have been investigated in the fresh water alga *Acetabularia* and they are thought to induce a

* *Present address:* Max Planck Institut für molekulare Pflanzenphysiologie Karl-Liebknecht-Str. 25, Haus 20 14476 Golm, Germany.

Correspondence to: J. Fisahn

defined orientation of the hairs within a whorl (Harrison, 1992). As a mechanism underlying this spatial pattern, a reaction diffusion system was suggested by Harrison (1992).

Many of the described pattern-forming mechanisms either affect transport proteins or are a direct consequence of the transport kinetics *per se* (Goodner & Quatrano, 1993). Therefore, the analysis of the spatial organization of transport proteins provides valuable information on the origins of pattern-forming mechanisms. This analysis is of particular importance when the kinetics of the transport proteins enable the development of a cellular polarity that might subsequently be interpreted by transcription factors which are involved in cellular expansion or differentiation.

In the present study, we report on experiments that were performed on isolated segments of a single *Chara* internodal cell. In particular, single illuminated acid transport domains were established and the extracellular current profile that developed within these segments was analyzed by a vibrating probe. A mathematical model was developed that simulated the acid and alkaline transport domains of *Chara* in terms of the transport kinetics associated with the H^+ transport protein. This model predicted the involvement of a reaction diffusion component that plays an essential role in establishing spatial control over H^+ transport along the *Chara* plasma membrane.

Materials and Methods

Culture Material

Culture material of *Chara corallina* Klein ex. Willd., em.R.D.W. (= *C. australis* R.Br.) was grown in the laboratory in 120-liter containers in solutions containing (mM): 3.0 Na^+, 0.3 K^+, 0.2 Ca^{2+}, 1.5 Cl^- and approximately 2.0 HCO_3^- (pH 9.0). Light from fluorescent lamps (cool white, Lifeline: Sylvania, Seneca Falls, NY) was employed (Fisahn & Lucas, 1992). The irradiance at the solution surface was 20 Wm^{-2} (measured using a silicon solar cell, Type No SO51OE7PL, International Rectifier, Los Angeles, CA).

Extracellular Current Measurements

Extracellular currents near the cell wall of internodal cells of *C. corallina* were measured by an improved vibrating probe system (Nuccitelli, 1986; Fisahn & Lucas, 1992). The protocol for the vibrating probe experiments has been described by Fisahn, McConnaughey & Lucas (1989). The tip of the voltage-sensing electrode was generally 10 μm in diameter, and this electrode was vibrated at a frequency of 294 Hz. The reference electrode was simply a large stationary Pt probe (100 μm in diam.) located 3 mm away from the point of current detection.

Cells were cut at noon and transferred to an artificial *Chara* pond water (CPW/B) containing (mM): 1.0 NaCl, 0.2 KCl, 0.2 $CaSO_4$, 1.0 $NaHCO_3$ (pH 8.2). For vibrating probe experiments, cells were pretreated overnight in CPW/B in 2-cm-deep Petri dishes.

For vibrating probe measurements, *Chara* internodal cells were mounted in Plexiglas chambers and placed on the stage of a Zeiss IM 405 inverted microscope (*see* Lucas, 1982). A fiber optic light source (KL 1500; Schott, Southbridge, MA) was used (lamp: EFR 150W-15V, GTE Products, Winchester, KY) to illuminate *Chara* cells during vibrating probe experiments. The fluence rate amounted to 20 Wm^{-2}. All experiments were conducted in temperature-controlled rooms at 25°C ± 1°C.

Subsequent to the recording of the current density profile along a single internodal cell, defined segments of this cell were covered with a metal sleeve (steel). This metal sleeve consisted of a hollow cylindrical tube with an inner diameter of 1.2 mm. After positioning of this tube, we were able to analyze the transport dynamics within a single illuminated acid transport domain.

Mathematical Modeling

Standard methods of numerical analysis were applied to analyze the *Chara* pattern-forming mechanism (Press et al., 1990). To solve the nonlinear differential equation used to model the pattern-forming mechanism of characean algal cells a shooting algorithm was applied (Acton, 1970). The set of differential equations that was developed to model the characean banding pattern is presented in the results section. A two-point boundary value problem emerged by the assumption of acidity (pH < 7) at both ends of a single *Chara* internodal cell (H > 0 in the transformed coordinate system that was used; *see* Appendix). This assumption has been validated in the majority of measured extracellular current profiles. The shooting method implements a multidimensional Newton-Raphson algorithm to improve the initial random guess of the model solution (Keller, 1968). For integrating the initial value problem a fourth-order Runge Kutta algorithm was incorporated into the numerical evaluation (Gear, 1971). The entire mathematical analysis was performed on a VAX computer at the University of Los Angeles, CA. Solutions of the iteration procedure were immediately plotted on the computer monitor and could be sent to a plotter.

Results

The specific mode that evolves into the steady-state pattern of acid and alkaline regions is influenced by the boundary conditions (Fisahn & Lucas, 1991) and by the length of the individual *Chara* cell. Since this spatial specialization of *Chara* membrane function is formed exclusively in the light, a reduction in the functional surface area was obtained by dark-adapting defined segments of the *Chara* internodal cells. Pronounced modifications in the extracellular current profile emerged when only a single acid domain was illuminated. A typical acid region that develops on the surface of *Chara* internodal cell is illustrated in Fig. 1*A*. This region of outwardly directed H^+ currents was obtained by dark adapting the adjacent acid and alkaline domains with a metal sleeve. Under these conditions, three alternative modes evolved inside this previously acid region (Fig. 1). These modes developed with equal probability and reflected adaptational mechanisms likely due to a diffusional process. However, the mode that developed in any particular experiment could not be predicted at the time of mounting the light barrier.

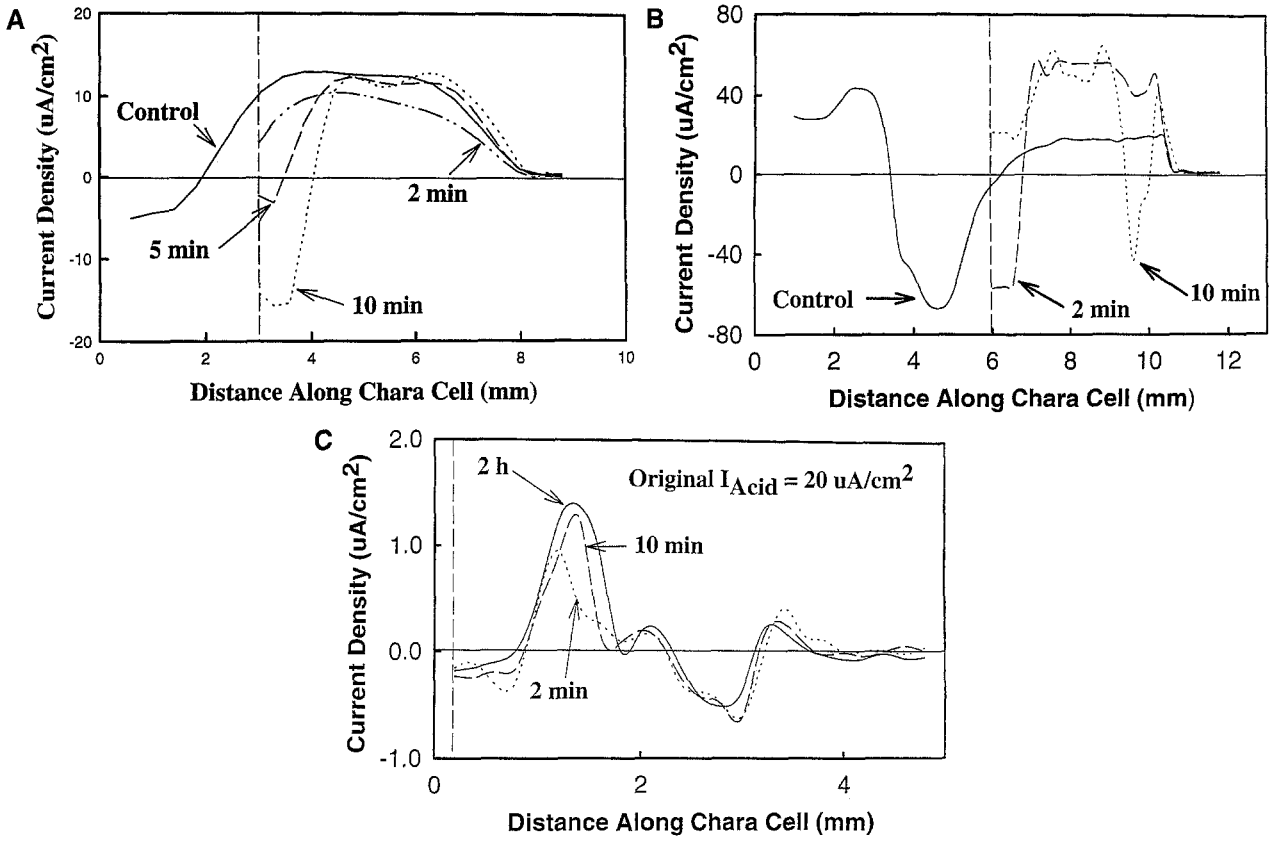

Fig. 1. (*A*) Before dark-adapting a defined segment of a *Chara* internodal cell, the extracellular current profile was measured. Only a portion of the profile is presented illustrating an acid region (continuous line); currents associated with the neighboring alkaline region are also depicted (negative current densities). Subsequently, a major part of the *Chara* cell was dark-adapted. The light screen that covered the *Chara* cell extended slightly into the original acid region. The vertical broken line indicates the position of the light barrier. The entire sector that is located to the left of this line was darkened while the segment to the right was exposed to an irradiance of 20 W/m^2. In this situation, a new alkaline region evolved inside of this previously acid segment. The final extracellular current profile obtained after 10 min remained stable for several hours. During adaption to the partial illumination of a single acid region various intermediate profiles emerged, which reflected the deactivation of the H^+ currents in the dark-adapted segments of the *Chara* cell (times indicate measurements taken after dark adaptation of defined *Chara* cell segments. (*B*) In this experiment, the light screen covered the left node and centrally located alkaline band of a *Chara* cell; an acid region located from 6–12 mm remained illuminated. Under these conditions, a second alkaline band evolved inside the original acid region (continuous line). As a consequence, the initial acid region was split into two acid and one alkaline domains. Similar to the previous situation, this new extracellular current profile remained stable for several hours. (*C*) After dark adapting the neighboring compartments, the extracellular current profile inside an initial acid region exhibited two alkaline and three acid domains. However, the current density inside the acid and alkaline regions was strongly reduced compared to the initial current densities (the uncovered initial acid region had a current density of 20 $\mu A/cm^2$).

The least complex mode that evolved inside an initial acid region was characterized by the formation of one novel alkaline domain (Fig. 1*A*) whose location resided directly adjacent to the dark-adapted cell section (number of repeats 20). During the formation of the steady-state current profile within the illuminated section, various intermediate states emanated. Most likely, this transitional phase reflected the deactivation associated with the transport proteins in the dark-adapted cell segment. Simultaneous to this dark-induced deactivation within the darkened cell segment, the extracellular current density along the illuminated region initially declined. However, this decrease only continued inside a limited sector close to the border of the barrier, giving rise to a new alkaline domain (Fig. 1*A*). In all experiments, the current densities associated with the acid domains that were investigated ranged between 10 $\mu A/cm^2$ and 40 $\mu A/cm^2$ (Fig. 1). No correlation between the absolute current density within an acid region and the pattern that evolved within this isolated region was observed.

Although identical experimental conditions were applied to other cells, a second and third mode evolved within the illuminated acid region. Whereas the first mode exhibited one acid region exclusively, the second mode displayed two acid- and one alkaline domain (Fig. 1*B;* number of repeats 20). A novel alkaline region developed in close proximity to the *Chara* nodal complex, in order to compensate for the outwardly directed H^+ currents associated with the acid regions. However, the

node itself faced an acid region. During the transition to a steady-state profile, a transient pattern occurred which resembled the first mode (*cf.* Fig. 1*A*).

With equal probability a third mode evolved inside the previously acid domain (Fig. 1*C;* number of repeats 20). However, this mode was characterized by a pronounced reduction in the magnitude of the extracellular current density. Although a steady-state pattern resulted, a significant asymmetry emerged that was not observed in measurements performed on completely illuminated *Chara* cells. A major acid domain, which developed close to the light-barrier, was not enclosed by an alkaline region. On the contrary, a minor acid region evolved in front of the neighboring alkaline domain (Fig. 1*C*).

Various mechanism have been analyzed in an attempt to explain the formation of biological patterns (Murray, 1989; Green, 1992). One class of these models focuses on a specific type of interaction between a diffusional and a reaction kinetic component that could give rise to a spatial pattern (Murray, 1989). Since various independent current profiles evolved within an illuminated acid region of *Chara,* it seems appropriate to assume that the pattern-forming mechanism of *Chara* is of a dynamic rather than of static origin. Our assumptions that will be used in the modeling imply that the kinetics of the H^+ transport protein associated with the acid and alkaline regions are of major importance for the pattern-generating mechanism.

The class of models that is used in the present approach is derived from the general conservation equation (Jackson, 1993).

$$(\partial/\partial t) \int_V H(x,t)\, dv = -\int_S J\, ds + \int_V f\, dv \qquad (1)$$

This equation says that the rate of change of the proton concentration ($H(x,t)$, with x spatial and t time variable) within the volume V is a function of the flow of protons (J) through the surface (S) of this volume. The variable f represents a possible proton source or a sink that is due to chemical reactions within the volume V. In our model, the volume V represents the inside of the *Chara* cell, S the plasma membrane, whereas the proton fluxes across the plasma membrane are described by the surface integral. Equation (1) is transformed by the application of the divergence theorem to the surface integral and the assumption of continuity for $H(x,t)$

$$\int_V [(\partial/\partial t)H + \nabla J - f(H,x,t)]\, dv = 0. \qquad (2)$$

The conservation of H in an arbitrary volume requires that

$$(\partial/\partial t)H + \nabla J = f(H,x,t). \qquad (3)$$

Since we want to consider diffusion of protons within the *Chara* cell wall

$$J = -D\, \nabla H, \qquad (4)$$

where D represents a diffusional coefficient. Introducing this Eq. (4) for classical diffusion (Jackson, 1993) into Eq. (3) results in

$$(\partial/\partial t)H = f + \nabla(D\, \nabla H). \qquad (5)$$

This type of differential equation has often been used to model distributions of chemicals (Turing, 1952).

One simplification of this equation arises by considering the steady state ($(\partial/\partial t)H = 0$). A second simplification emerges from considering one dimension only. The reaction kinetic component (f) of our model then has to reflect the nonlinear kinetic characteristics for the H^+ currents mediated by the H^+-transporter that has been analyzed in a previous study (Fisahn, Hansen & Lucas, 1992). The mathematical expression describing this reaction kinetic component was earlier derived based on experimental data obtained using a vibrating probe technique (Fisahn et al., 1992). When the extracellular pH value was lowered, a decline in the inwardly directed H^+ currents within the alkaline regions resulted. This inverse relation between H^+ inward current and the extracellular pH gave rise to a specific nonlinearity and probably to the spatial organization of acid and alkaline domains.

In addition to this experimentally derived mathematical expression for the H^+ current (Fisahn et al., 1992) the diffusional component completed the mathematical model (as seen in Eqs. 1–5). Thus H^+ diffusion in the extracellular matrix controls the directionality associated with inwardly and outwardly directed H^+ currents within the alkaline and acid regions, respectively. In mathematical terms, these assumptions establish a nonlinear differential equation.

$$d^2H/dx^2 = -I, \text{ for all pH} < 7 \qquad (6)$$

$$d^2H/dx^2 = I, \text{ for all pH} > 7 \qquad (7)$$

(H: proton concentration at the surface of a *Chara* cell; x: length along the *Chara* cell surface, spatial variable, I(= const) reaction kinetic component that describes the proton sinks and sources which are generated by the H^+ transport protein; in Eq. (5) this component is represented by the general function f).

Together with the two-point boundary conditions that impaired acidity at both nodal ends a complete mathematical problem was established (pH < 7 at $x = 0$ and x = L; L: length of the *Chara* internodal cell; *see* Appendix). This reaction diffusion system was analyzed using numerical analysis (Keller, 1968; Acton, 1970). Numerical solutions resulted in a pH profile identical to that obtained experimentally (Fig. 2). Obviously, the two-point boundary problem provided a solution that reflected the pH banding pattern previously measured

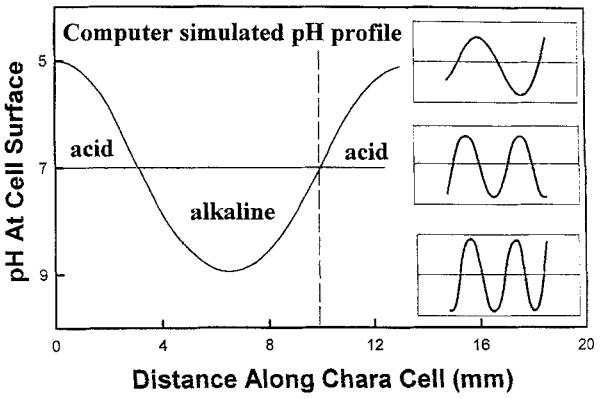

Fig. 2. To establish the diffusional component of the *Chara* growth pattern, a reaction diffusion model of this system was simulated on the computer. The solutions obtained (continuous line) reflect the *Chara* banding pattern and exhibit alternating acid and alkaline domains. Lucas and Nuccitelli (1980) have demonstrated that the acid regions exactly reflect the regions of outwardly directed currents. A similar correlation holds for the alkaline regions and the inwardly directed currents. Further computer simulations focused on the acid region that resides on the right side of the broken vertical line. Inside this acid region, various secondary pH-profiles evolved as a function of the boundary conditions used in the computer simulation (insets). These modes resembled the measured profiles evolving from partially illuminated *Chara* cells.

along a single *Chara* cell (Lucas, 1982; Fig. 2). Furthermore, the solution completely met the imposed requirements of acidity at both nodal ends (two-point boundary condition).

In the mathematical model, we simulated the light barrier situation as a shift in the boundary conditions (Fig. 2). Therefore, we reduced the length of the *Chara* cell within the model. The actual boundary conditions that were used are illustrated in the various solutions (Fig. 2). The reaction diffusion system thus generated secondary pH profiles within the remaining illuminated acid region in response to such a change in the *Chara* spatial domain. Depending on the initial conditions, the model demonstrated that various modes could evolve inside this acid domain. As indicated in Fig. 2, adjustments in the boundary conditions used in the model yielded several modes within the previously acidic transport domain.

Discussion

When a defined amount of a *Chara* cell was dark adapted, new alkaline regions were formed inside what were previously acid regions (Figs. 1*A–C*, and 2). Since a single isolated acid region was illuminated and, thus an unstable configuration was established, the *Chara* cell was forced to accommodate to this imposed constraint. The underlying mechanism responsible for the emergence of the new pattern cannot result from structural differences within a previously acid region, since several modes evolved inside such an acid domain. Based on these results, spatial organization of transport proteins, involving a reaction-diffusion component, provides a simple but profound explanation for this phenomenon. Support for this hypothesis emerged from mathematical modeling, which enabled us to simulate the *Chara* current pattern (Fig. 2). The unique assumption required by the mathematical model involved a specific nonlinear transport characteristic that controls the transport properties of the H^+-transport system across the *Chara* plasma membrane.

The emergence of spatial patterns by diffusing chemicals that are capable of interaction has already been suggested by Turing (1952). Such a development of spatially inhomogenous patterns involving diffusion and a reaction kinetic component seemed a completely novel concept at this time. However, from then on a great amount of work focused on these mechanisms and their implications on biological pattern formation (Swindale, 1980; Nagorcka, 1986, 1988; Murray, 1989; Wolpert, 1969, 1971, 1981). Similar to the situation discussed for the H^+ diffusion along the *Chara* surface, diffusion driven instabilities are involved in all of these pattern forming mechanisms (Levin & Segel, 1985). For *Chara,* this diffusion driven instability is absent in the dark and thus a stable steady-state is established that is insensitive to small perturbations in the H^+ distribution. However, upon illumination diffusion of H^+ occurs in the extracellular space giving rise to diffusion driven instabilities in the transport of H^+ across the *Chara* plasma membrane (Lucas, 1982; Fisahn et al., 1992). This diffusion driven instability in the H^+ distribution enables the formation of acid and alkaline regions along the *Chara* cell surface (Murray, 1989).

The light barrier experiments provide circumstantial evidence that diffusion of H^+ along the *Chara* surface and transport of H^+ across the *Chara* plasma membrane interact in the specific manner described by the proposed mathematical model. Subsequent to the darkening of defined *Chara* segments, the diffusion profile along the *Chara* surface will be perturbed within the illuminated region (Fig. 1*A–C*). This perturbation in H^+ diffusion will affect the transport events inside the previously illuminated acid region. Therefore, local perturbations in the H^+ distribution within the original acid region will be the consequence. These local perturbations in the H^+ concentration might easily amount to values close to or beyond the critical H^+ concentration that triggers a transition from H^+ export to H^+ input (Fisahn et al., 1992). Thus, new alkaline domains will be established within the previously acid region. Since diffusion is a random process, it cannot be predicted at the onset of an experiment at which locations within the illuminated acid region these critical H^+ concentrations will be obtained.

For these reasons the emergence of several modes is in line with the predictions of our model (Fig. 2).

The development of several modes inside an original acid region of *Chara* indicates that the spatial separation of acid and alkaline regions seems to be of self-organized origin (Murray, 1989). Obviously, this type of adaptation provides great advantage compared to a statically fixed structure (Benjacob et al., 1992). Moreover, this flexibility enables the *Chara* cell to establish acidic regions for cell expansion growth even under unfavorable conditions (Metraux, Richmond & Taiz, 1980). In terms of carbon partitioning the expanding cell wall provides a sink element that might be required to maintain an optimal carbon allocation pattern (Carpita & Gibeaut, 1993). The allocation of carbon is linked to the uptake of carbon at the level of the plasma membrane. Adaptation of acid regions might thus function in regulating carbon uptake and therefore transport of HCO_3^- and CO_2 across the *Chara* plasma membrane and adjusting these transport rates to the imposed constraints (Lucas, 1983).

This work was supported by the Deutsche Forschungsgemeinschaft (grant #571 1/1) to JF.

References

Acton, F.S. 1970. Numerical Methods that Work. Harper and Row, New York.

Benjacob, E., Shmueli, H., Schochet, O., Tenebaum, A. 1992. Adaptive self-organization during growth of bacterial colonies. *Physica A.* **187:**378–424

Carpita, N.C., Gibeaut, D.M. 1993. Structural models of primary cell walls in flowering plants: consistency of molecular structure with physical properties of the walls during growth. *Plant J.* **3:**1–30

Fisahn, J., McConnaughey, T., Lucas, W.J. 1989. Oscillations in extracellular current, external pH and membrane potential and conductance in the alkaline bands of *Nitella* and *Chara. J. Exp. Bot.* **40:**1185–1193

Fisahn, J., Lucas, W.J. 1990*a*. Inversion of extracellular current and axial voltage profile in *Chara* and *Nitella. J. Membrane Biol.* **113:**1–8

Fisahn, J., Lucas, W.J. 1990*b*. Effects of microtubule-specific agents on the spatial and electrical properties of the plasma membrane in *Chara corallina. Planta* **182:**506–512

Fisahn, J., Lucas, W.J. 1991. Autonomous local area control over membrane transport in *Chara* internodal cells. *Plant Physiol.* **95:**1138–1143

Fisahn, J., Lucas, W.J. 1992. Direct measurement of the reversal potential and current-voltage characteristics in the acid and alkaline regions of *Chara corallina. Planta* **186:**241–248

Fisahn, J., Hansen, U.P., Lucas, W.J. 1992. Reaction kinetic model of the *Chara* plasma-membrane 2 cycle H^+-ATPase. *Proc. Natl. Acad. Sci. USA* **89:**3261–3265

Gear, C.W. 1971. Numerical Initial Value Problems in Ordinary Differential Equations. Prentice Hall, Englewood Cliffs, NJ

Goodner, B., Quatrano, R. 1993. *Fucus* embryogenesis: a model to study the establishment of polarity. *Plant Cell* **5:**1471–1481

Green, P.B. 1992. Pattern formation in shoots — a likely role for minimal energy configurations of the tunica. *Int. J. Plant Sci.* **153:**59–75

Harrison, L.G. 1992. Reaction-diffusion theory and intracellular differentiation. *Int. J. Plant Sci.* **153:**76–85

Jackson, J.D. 1993. Classical Electrodynamics. DeGruyter, Berlin

Jaffe, L.F. 1977. Electrophoresis along cell membranes. *Nature* **265:**600–602

Jaffe, L.F. 1981. The role of ion currents in establishing developmental gradients *In:* International Cell Biology. H.G. Schweiger, editor. pp. 507–511

Jaffe, L.F., Nuccitelli, R. 1977. Electrical controls of development. *Ann. Rev. Biophys. Bioeng.* **6:**445–476

Keller, H.B. 1968. Numerical Methods for Two-Point Boundary-Value Problems. Blaisdell, Waltham, MA

Levin, S.A., Segel, L.A. 1985. Pattern generation in space and aspect. *SIAM Rev.* **27:**45–67

Lucas, W.J. 1982. Mechanism of acquisition of exogeneous bicarbonate by internodal cells of *Chara corallina. Planta* **156:**181–192

Lucas, W.J. 1983. Photosynthetic assimilation of exogeneous HCO_3^- by aquatic plants. *Annu. Rev. Plant Physiol.* **34:**71–104

Lucas, W.J., Nuccitelli, R. 1890. HCO_3^- and OH^- transport across the plasmalemma of *Chara:* spatial resolution obtained using extracellular vibrating probe. *Planta* **150:**120–131

Metraux, J.P., Richmond, P.A., Taiz, L. 1980. Control of cell elongation in *Nitella* by endogenous cell wall pH gradients. Multiaxial extensibility and growth studies. *Plant Physiol.* **65:**204–210

Murray, J.D. 1989. Mathematical Biology. Springer-Verlag, Berlin

Nagorcka, B.N. 1986. The role of a reaction-diffusion system in the initiation of skin organ primordia. I. The first wave of initiation. *J. Theor. Biol.* **121:**449–475

Nagorcka, B.N. 1988. A pattern formation mechanism to control spatial organization in the embryo of *Drosophila melanogaster. J. Theor. Biol.* **132:**277–306

Nuccitelli, R. 1986. A two dimensional vibrating probe with a computerized graphics display. *In:* Ionic Currents in Development. R. Nuccitelli, editor. pp. 13–20. Alan R. Liss, New York

Press, W.H., Flannery, B.P., Teukolsky, S.A., Vetterling, W.T. 1990. Numerical Recipes in C. Cambridge University Press, Cambridge

Quatrano, R.S. 1978. Development of cell polarity. *Ann. Rev. Plant Phys.* **29:**487–510

Quatrano, R.S. 1990. Polar axis fixation and cytoplasmic localization in *Fucus. In:* Genetics of Pattern Formation and Growth Control. pp. 31–46. Wiley-Liss, New York

Smith, F.A., Walker, N.A. 1976. Chloride transport in *Chara corallina* and the electrochemical potential difference for hydrogen ions. *Exp. Bot.* **27:**451–459

Spanswick, R. 1981. Electrogenic ion pumps. *Annu. Rev. Plant Physiol.* **32:**267–289

Spear, D.G., Barr, J.K., Barr, C.E. 1969. Localization of hydrogen ion and chloride fluxes in *Nitella. J. Gen. Physiol.* **54:**397–414

Swindale, N.V. 1980. A model for the formation of ocular dominance stripes. *Proc. Roy. Soc. Lond.* **B208:**243–264

Turing, A.M. 1952. The chemical basis of morphogenesis. *Phil. Trans. Roy. Soc. Lond.* **B237:**37–72

Wagner, V.T., Brian, L., Quatrano, R.S. 1992. Role of a vitronectin-like molecule in embryo adhesion of the brown alga *Fucus. Proc. Natl. Acad. Sci. USA* **89:**3644–3648

Wolpert, L. 1969. Positional information and the spatial pattern of cellular differentiation. *J. Theor. Biol.* **25:**1–47

Wolpert, L. 1971. Positional information and pattern formation. *Curr. Top. Dev. Biol.* **6:**183–224

Wolpert, L. 1981. Positional information and pattern formation. *Phil. Trans. Roy. Soc. Lond.* **B295:**441–150

Appendix

The solution for either of the second order differential Eqs. (6) or (7) may be written in the form:

$$H = (1/2)\, Ix^2 + bx + c, \qquad \text{(A1)}$$

if we assume for simplicity that I is a constant. Setting the parameters b and c equal to zero this solution represents a parabola (Fig. A1*A*). Depending on the sign (+, −) of the quadratic term (x^2), this parabola is open to the positive or the negative H-direction (Fig. A1*A*). The observed modes of the *Chara* banding pattern might be a consequence of the absolute value of the parameter I in Eq. (A1) (Fig. A1*B*). Furthermore, the origin of the parabola can be shifted in the direction of positive or negative H values by allowing the parameter c to take positive or negative values (Fig. A1*B*). To further simplify the numerical analysis, we performed a transformation of the coordinate system by transforming neutral pH (7) to 0. Under these assumptions, it becomes obvious that the alignment of parabolas with alternating positive and negative openings can be used to model the alternating acid and alkaline regions of the *Chara* banding pattern (Fig. A1*C*). Numerical solutions of the complete set of differential Eqs. (6) and (7) have been presented in the results section.

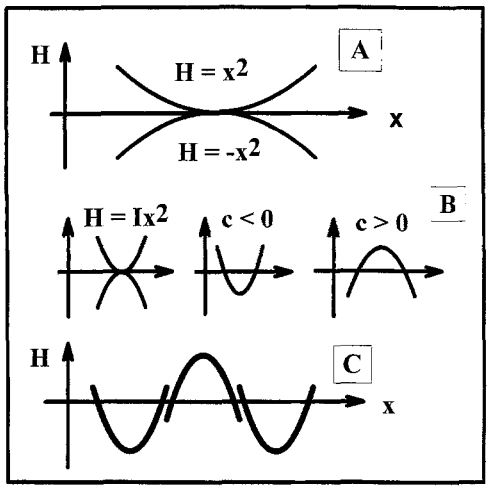

Fig. A1. Solutions of the differential Eqs. (6) and (7). Details are described in the appendix.

In a previous study, we demonstrated that the transport protein that mediates the acid and alkaline regions of *Chara* can function in an H^+ input and an H^+ output mode (Fisahn, Hansen & Lucas, 1992). If this protein is activated in the H^+ import mode, the diffusion of H^+ along the *Chara* surface is described by Eq. 7 (Fig. A2*A*). By a modification of the extracellular pH, the export mode could be switched into the input configuration (Fisahn & Lucas, 1990*a*). Therefore, a second diffusional equation is required that determines diffusion in this situation (i.e., Eq. (6)); Fig. A2*B*). The combined effect of these diffusional processes will then give rise to the spatial pattern along the *Chara* cell surface.

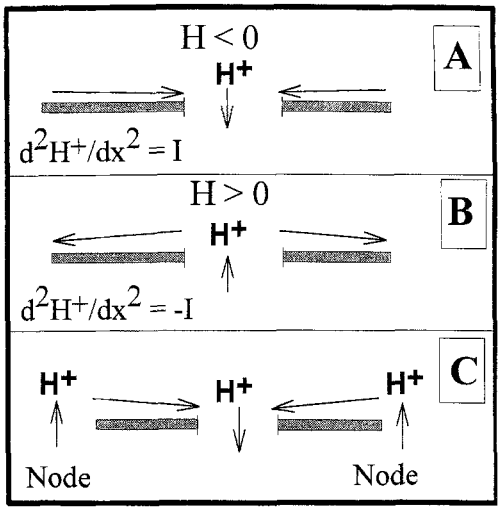

Fig. A2. (*A*) Diffusion of H^+ into the cytoplasm gives rise to Eq. 7. (*B*) Diffusion out of the acid regions provides Eq. 6. (*C*) For the modeling, increased H^+ concentrations were assumed at the nodal ends. The shaded areas indicate the *Chara* plasma membrane.

To analyze these diffusion equations numerically, boundary conditions are required. As indicated in Fig. A2*C*, we used the assumption of acidity at both nodal ends of a *Chara* cell. However, these boundary conditions are not essential in that every other set of boundary conditions would also have resulted in a spatial pattern. Since experiments very often showed that the nodal regions were acid we selected these conditions for our model.